NeuroImage 53 (2010) 1126–1134

Contents lists available at ScienceDirect

NeuroImage

journal homepage: www.elsevier.com/locate/ynimg

# Genetics of primary cerebral gyrification: Heritability of length, depth and area of primary sulci in an extended pedigree of Papio baboons

P. Kochunov [a,*], D.C. Glahn [a], P.T. Fox [a], J.L. Lancaster [a], K. Saleem [b], W. Shelledy [c,d], K. Zilles [e], P.M. Thompson [f], O. Coulon [g], J.F. Mangin [h], J. Blangero [c], J. Rogers [c,d]

[a] Research Imaging Institute, The University of Texas Health Science Center, San Antonio, TX 78229, USA
[b] Department of Anatomy and Neurobiology, Washington University School of Medicine, St. Louis, MO, USA
[c] Department of Genetics, Southwest Foundation for Biomedical Research, San Antonio, TX 78227, USA
[d] Southwest National Primate Research Center, San Antonio, TX 78227, USA
[e] Institute of Neuroscience and Biophysics, INB-3 and JARA, Research Centre Jülich, Jülich, Germany
[f] Laboratory of Neuro Imaging, UCLA School of Medicine, Los Angeles, CA, USA
[g] Laboratoire des Sciences de l' Information et des Systèmes, UMR 6168, Marseille, France
[h] Service Hospitalier Frédéric Joliot, CEA, Orsay, France

ARTICLE INFO

*Article history:*
Received 24 July 2009
Revised 7 December 2009
Accepted 9 December 2009
Available online 24 December 2009

ABSTRACT

Genetic control over morphological variability of primary sulci and gyri is of great interest in the evolutionary, developmental and clinical neurosciences. Primary structures emerge early in development and their morphology is thought to be related to neuronal differentiation, development of functional connections and cortical lateralization. We measured the proportional contributions of genetics and environment to regional variability, testing two theories regarding regional modulation of genetic influences by ontogenic and phenotypic factors. Our measures were surface area, and average length and depth of eleven primary cortical sulci from high-resolution MR images in 180 pedigreed baboons. Average heritability values for sulcal area, depth and length ($h^2_{Area} = .38 \pm .22$; $h^2_{Depth} = .42 \pm .23$; $h^2_{Length} = .34 \pm .22$) indicated that regional cortical anatomy is under genetic control. The regional pattern of genetic contributions was complex and, contrary to previously proposed theories, did not depend upon sulcal depth, or upon the sequence in which structures appear during development. Our results imply that heritability of sulcal phenotypes may be regionally modulated by arcuate U-fiber systems. However, further research is necessary to unravel the complexity of genetic contributions to cortical morphology.



## Introduction

Although the genetic control of primary gyrification is an area of active research, little is known about the genetic contribution to intersubject variability of cerebral landscape. The evolution of the primate brain provides, perhaps, the best evidence that cortical morphology is strongly influenced by genetic factors (Tamraz and Comair, 2006). During evolution, newly derived primate groups such as anthropoid and hominoid primates developed larger, more gyrified brains (Martin et al., 2007; Preuss, 2007; Welker, 1990). Yet, the gyrification pattern of the cerebral cortex across primates is recognizable by the pattern of morphological features, called primary cortical structures, that are conserved across different primate species (Tamraz and Comair, 2006). Primary gyrification begins in early stages of telencephalic development (Tamraz and Comair, 2006) as its onset coincides with completion of neuronal proliferation and migration and progression is accompanied by an explosive increase in cerebral growth (Armstrong et al., 1991, 1995; Pillay and Manger, 2007). The onset of primary gyrification also coincides with the onset of neuronal differentiation, a developmental process that partitions the cortical ply into an intricate mosaic of specialized functional areas (Neal et al., 2007). In Old World monkeys, apes and humans, cortical sulci and gyri appear during primary gyrogenesis in a tightly controlled ontogenic sequence (Armstrong et al., 1995; Pillay and Manger, 2007; Zilles et al., 1989). Primary gyrogenesis is completed before birth, and is followed by the myelination of cortical axons (Armstrong et al., 1991, 1995). In contrast, secondary and tertiary gyrification, more prominent in higher primates such as hominoid apes and humans, accompany postnatal cerebral growth and myelination, giving the brain its adult appearance (Tamraz and Comair, 2006).

The ontogenic order of appearance of primary cortical structures has been extensively studied and is found to be similar among humans and nonhuman primates (Armstrong et al., 1995; Pillay and Manger, 2007; Zilles et al., 1989). The order in which primary structures make their appearance is putatively related to such

* Corresponding author. Fax: +1 210 567 8152.
*E-mail address:* kochunov@uthscsa.edu (P. Kochunov).

1053-8119/$ – see front matter © 2009 Elsevier Inc. All rights reserved.
doi:10.1016/j.neuroimage.2009.12.045

developmental processes as neuronal differentiation, development of functional associations and hemispheric lateralization (Galaburda and Pandya, 1982; Van Essen, 1997; Welker, 1990). Neurophysiological studies have long considered primary structures as the spatial landmarks and boundaries that form the intricate cortical mosaic of functional areas (Brodmann, 2005; Rademacher et al., 1993, 2001a,b). Functional and anatomical studies in humans also established a clear pattern of function–structure relationships among primary cortical structures and functional areas. However, the extensive secondary and tertiary gyrification of the human cortex make these associations more complex in humans than in nonhuman primates (Fischl et al., 2007; Van Essen, 2004).

Sources of individual morphological variability of the cortical landscape within a given primate species are not well understood. Detailed explanation of the causes and consequences of morphological variation in brain structure could have wide significance and numerous implications for neuroscience, psychology and psychiatry as well as for evolutionary biology. The first step in this direction is to study the proportion of individual variance that can be explained by genetic differences among related individuals. This measurement, called heritability ($h^2$), is defined as the proportion of total phenotypic variance ($\sigma^2_p$) that is explained by additive genetic factors ($\sigma^2_g$) (Eq. 1).

$$h^2 = \frac{\sigma^2_g}{\sigma^2_p} \quad (1)$$

High heritability has already been established for a number of neuroimaging-based phenotypes such as total brain size, gray matter volume, regional gray matter thickness, length of the corpus callosum and volume of cerebral ventricles (see Thompson et al., 2001 for a review). In our recent analyses in one nonhuman primate species (baboons, *Papio hamadryas*) we found high heritability for brain volume ($h^2=.86$; $p<1e-4$), gray matter volume ($h^2=.67$; $p=.01$) and cortical surface area ($h^2=.73$; $p<1e-3$) (Rogers et al., 2007). The work presented here is an extension of our previous research with the goal of measuring the contribution of intersubject genetic differences to *regional* variation in the degree of cerebral gyrification.

Several studies report high heritability estimates for phenotypes describing regional cortical morphology (Cheverud et al., 1990; Hulshoff Pol et al., 2006; Le Goualher et al., 2000; Lohmann et al., 1999, 2007; Thompson et al., 2002). The degree of genetic contribution to cortical morphology varies across the brain. To explain these findings, two theoretical models have been proposed, but not formally tested. The first model, suggested by a study by Cheverud and colleagues (1990), draws a connection between developmental factors such as prenatal neurohormonal environment and the genetic versus environmental contributions to variability in the length of cortical sulci. Using an innovative approach and measuring endocranial casts from free-ranging rhesus macaques, Cheverud and colleagues (1990) found progressively lower heritabilities for the length of the primary sulci that appear later in cerebral development. This implied that lower heritability for later-appearing sulci may be due to higher contributions of environmental factors to the overall phenotypic variance across animals. They suggested that higher environmental contribution to sulcal morphology could be due to changes in prenatal hormone-mediated neurohumoral environment and tissue receptivity, which become progressively more variable during development (Cheverud et al., 1990). A trend toward higher heritability values for primary cortical structures appearing earlier in development was also reported in humans (Brun et al., 2008; Chiang et al., 2008; Le Goualher et al., 2000; Lohmann et al., 2007, 1999).

The second theoretical model, proposed by Lohmann and colleagues (1999), suggests that the genetic versus environmental contributions to morphological variability are modulated by sulcal depth, with deeper primary sulci under more genetic control than shallower structures. In their study of cortical variability in human twin-pairs, Lohmann and colleagues observed that the deepest of the cortical structures appeared to be the least affected by the environmental component of the "macromechanical forces" directing the postnatal brain growth and development. This conclusion was based in part on theories of cerebral gyrification, which postulate that the depth of individual sulci is influenced by mechanical tensions in the underlying white matter tracts (Van Essen, 1997; Welker, 1990). Under this model, deeper cortical sulci are postulated to be formed earlier during development due to greater tension between a specific sulcal fundus and the other cortical structures to which it is "anchored" by underlying white matter tracts. Greater mechanical tension responsible for the formation of deeper sulci was thus suggested to be the reason for higher inter-twin similarity observed in these structures (Lohmann et al., 1999, 2008).

The goal of this study is to formally test the two proposed theoretical models of genetic contribution to variation in cerebral gyrification. Neither of these proposed models was fully tested by the original authors due to methodological limitations in each analysis. The innovative study by Cheverud et al. (1990) measured sulcal length indirectly from the endocranial casts, based on the bony impressions on the inner surface of the cranial cavity. This limited their analysis to cortical sulci with corresponding endocranial impressions, excluding many sulci from the limbic, parietal and occipital lobes. Another limitation was that heritability estimates were calculated based on incomplete pedigree information, since the dam but not the sire was known for each study individual (Cheverud et al., 1990). The study by Lohmann et al. (1999) had limited numbers of subjects (only 19 twin-pairs), preventing them from directly calculating the genetic contribution to sulcal variability. Instead, genetic contribution was indirectly estimated as the ratios of the within versus across twin-pairs variance. Despite not being formally tested, the proposed hypotheses have been used to explain findings in normal cortical variability and disease-specific differences observed in disorders such as bipolar depression and schizophrenia (Cykowski et al., 2008a,b; Fornito et al., 2007; Harris et al., 2004; Narr et al., 2004). This study was designed to overcome these limitations, while analyzing a comparable set of phenotypes.

In the current study, we measure sulcal area, length and depth from high-resolution MR imaging from 180 pedigreed *Papio* baboons (*Papio hamadryas*). *Papio* baboons are uniquely suited among nonhuman primates for translational neuroimaging genetic research. Phylogenetically, *Papio* baboons and other cercopithecoids (Old World monkeys), are more closely related to humans than all other primates, with the exception of ape (hominoid) species (Stewart and Disotell, 1998). *Papio* baboons express all primary cortical structures, but do not develop prominent secondary/tertiary anastomotic sulci. In apes and humans, anastomotic sulci often interfere with and/or interrupt the spatial course of the primary sulci, thus artificially increasing morphological variability and complicating phenotypic analysis. From a neuroimaging prospective, *Papio* baboons have the largest brains of any commonly studied laboratory primate except chimpanzees, which are apes and have more prominent secondary cortical sulci. The average cerebral volume in adult baboons (~180 $cm^3$) is more than twice that of adult rhesus macaques or cynomolgus macaques (Leigh, 2004; Leigh et al., 2003; Martin, 1990; Rogers et al., 2007).

## Methods

### *Animal subjects*

One hundred eighty adult *Papio* baboons (olive baboons, *Papio hamadryas anubis*, and yellow baboons *P. h. cynocephalus* and their hybrids) including 68 males and 112 females were selected from the large multigeneration pedigreed colony of more than 2000 baboons

maintained by the Southwest National Primate Research Center at the Southwest Foundation for Biomedical Research (SFBR) in San Antonio, TX. The average age of the study animals was 16.0 ± 4.2 years [range: 7–28 years]. This age range was chosen to minimize the effects of development or senescence based on studies of cerebral ontogeny (Leigh, 2004; Leigh et al., 2003). The genealogical relationships among study animals included 414 parent-offspring pairs, 51 full sib pairs, 645 half-sib pairs, and a large number of more distant kinship relationships.

*Animal handling and MR imaging*

Handling, anesthesia and imaging protocol used in this study are detailed elsewhere (Kochunov and Duff Davis, 2009; Rogers et al., 2007). In short, high-resolution (isotropic 500 μm), T1-weighted images were acquired using a 3D IR-TurboFlash sequence optimized for anatomical imaging of baboon brain. An adiabatic inversion recovery (IR) contrast pulse with linear phase encoding schema was employed primarily because it led to a uniform tissue contrast across the imaging volume (being less affected by B1-inhomogeneity/RF penetration artifacts). The sequence control parameters (FOV = 128 mm, TI = 795 ms, TE = 3.04, $TR_1$ = 5 ms, $TR_2$ = 2000 ms and flip angle = 10°) were modeled to produce GM/WM contrast of 25% based on the analytical solutions to Bloch equations (Deichmann et al., 2000) and average measured values of T1, T2 and PD. The model-determined imaging sequence parameters were verified in a group of 5 animals, where group-average WM-GM contrast was calculated to be 25.2 ± 2% (range: 22–26%). Image acquisition was performed using a retrospective motion-corrected protocol (Kochunov et al., 2006). Under this protocol, six full resolution segments, 9 min long each, were acquired for a total sequence running time of ~54 min.

*Image processing and analysis*

The image processing pipeline consisted of the following steps: removal of non-brain tissue, correction for spatial variations in intensity due to scanner radio-frequency inhomogeneity and global spatial normalization to a population-based template to reduce global variability in brain size and orientation (Rogers et al., 2007) (Fig. 1A and B). Next, object-based-morphology (OBM) methods were used to characterize individual cortical variability (Kochunov et al., 2005; Mangin et al., 2003). The OBM approach is a recognition model that parcelates the cortical landscape into objects representing the regional in-folding (sulci) and out-folding (gyri) (Mangin et al., 2003). OBM characterizes gyral and sulcal variations by parcellating the cortex into simple 2D surfaces. During OBM processing pial and gray matter/white matter interfaces are reconstructed from the tissue segmented image (Fig. 1C–F). A "crevasse detector" is used to delineate the shape of the individual sulcal surfaces based on topological criteria (Fig. 1G). Topologically, a sulcal surface is defined as the 2D surface that passes midway between the opposing gyral banks. The sulcal surface spans the entire space contained in a sulcal fold, from the most internal portion (the fundus) and its intersection with the local convex hull of the overall "brain envelope" surface (the top ridge). The sulcal surface can be conceived as the skeleton of the CSF volume contained between the two opposing gyral walls that form the sulcal fold (Mangin et al., 1995, 2004). In the final step, sulcal structures are identified and labeled (Fig. 1H).

*Measuring sulcal length, depth and area*

One composite measurement (surface area) and two linear measurements (sulcal length and depth) were made for each of the sulci shown in Table 1 in every study animal. As shown in Fig. 2, a sulcal structure is defined by its exterior boundary (top ridge), interior boundary (fundus) and a surface composed of the loci that are equidistantly located from the opposing gyral banks that formed the sulcal fold. The composite measurement, sulcal area, was calculated as the area of the sulcal surface. Sulcal length and depth were measured using previously published methods (Cykowski et al., 2008a) (Fig. 2). In short, each sulcal surface was parameterized using a heat diffusion

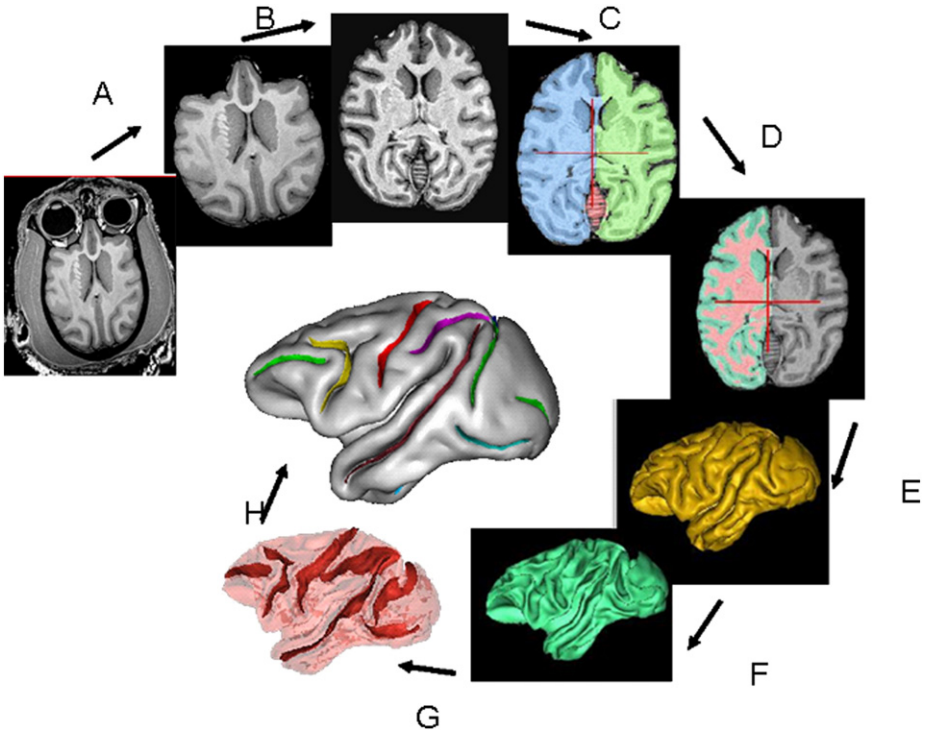


**Fig. 1.** Structural MRI data were processed using object-based-morphometry pipeline. Brain images were processed with the following steps: skull-stripping (A); RF-homogeneity correction and spatial normalization (B); hemispheric and tissue segmentation (C, D), extraction of GM and WM surfaces (E, F); Identification of sulcal surfaces using crevasse detector (G); Identification and labeling of sulcal structures (H).

**Table 1**
Name (label), area, depth, length: average + standard error (standard error after correcting for covariates) for 11 primary sulci of baboon brain.

| Sulcal name (label)[a] | Area ($mm^2$) | Depth (mm) | Length (mm) | ED[b] | Functional areas associated with a given structure[c] |
|---|---|---|---|---|---|
| Arcuate (ar) | 349.2 ± 54.3 (53.1) | 10.8 ± 1.1 (1.03) | 34.3 ± 3.8 (3.7) | 120 | Superior ar: anchors: BA8 (B/AD); inferior ar: separates: anterior bank BA45B, posterior bank BA44, 47. |
| Cingulate (cgs) | 478.1 ± 75.2 (71.6) | 9.7 ± 1.0 (.96) | 54.4 ± 5.1 (4.9) | 100 | Superior bank: BA10, 9/32, 8/32, 6/32, 3A, PECg, 2; inferior bank: BA32,24,23,31 |
| Central (cs) | 508.1 ± 53.7 (52.6) | 11.9 ± 0.7 (0.7) | 43.4 ± 2.8 (2.7) | 90 | Anterior bank: BA4; posterior bank: BA1-2; fundus: BA3a/b |
| External-Calcarine calcarine (ecal) | 201.1 ± 64.4 (62.4) | 7.6 ± 1.8 (1.7) | 26.3 ± 3.6 (3.4) | 100 | Houses V1 area |
| Inferior occipital (ios) | 319.9 ± 68.3 (63.3) | 9.5 ± 1.4 (1.4) | 32.7 ± 4.5 (4.1) | 110 | Houses V4 area |
| Occipital-temporal (ots) | 264.3 ± 62.0 (59.7) | 6.2 ± 1.4 (1.3) | 42.3 ± 8.2 (8.0) | 120 | Houses TF area |
| Inferior parietal (ips) | 710.3 ± 82.0 (82.1) | 19.1 ± 1.6 (1.5) | 34.5 ± 3.3 (3.2) | 100 | Anterior bank: BA5; posterior bank: BA7,LIP; fundus: VIP, AIP |
| Parietal-occipital (pos) | 437 ± 95.0 (94.5) | 15.3 ± 2.5 (2.5) | 32.5 ± 6.1 (6.0) | 80 | Anterior bank: BA7, PO; Posterior posterior bank: V2/3; fundus: PIP |
| Lunate (lu) | 620 ± 88.0 (84.3) | 16.4 ± 2.1 (1.9) | 38.8 ± 3.6 (3.5) | 100 | Anterior bank: V3/4; Posterior posterior bank: V2 |
| Principal (ps) | 230.9 ± 46.1 (42.0) | 8.8 ± 1.3 (1.2) | 26.1 ± 3.5 (3.3) | 110 | BA46 |
| Superior-temporal (sts) | 1237.8 ± 102.1 (97.4) | 17.3 ± 1.1 (1.0) | 72.5 ± 3.6 (3.4) | 90 | Superior bank: TPP, TPO, V5; inferior bank: TE, V4; fundus: PGa/IPa |

[a] Naming and labeling convention was taken from Saleem and Logothetis (2007).
[b] Embryological day of appearance (ED) was taken from Fukunishi et al. (2006).
[c] Cytoarchitectonic information was taken from Saleem and Logothetis (2007).

model. Sulcal surface features consisting of (1) the fundus, (2) the exterior boundary and (3) the poles where two ridges meet are used as heat sources creating a gradient of heat along the sulcal surface. A system of second order differential equations is numerically solved to calculate a distribution of temperatures along the sulcal surface (Coulon et al., 2006). A 2D ($x$, $y$) coordinate system is then created by fitting isothermal lines along and normal to the direction of sulcal fundus and top ridge. The length of the sulcus was defined as the average length of 100 isothermal curves uniformly placed along the sulcal surface, continuously collinear with the fundus and the top ridge. The length of the isothermal curves was calculated by fitting the points on the isothermal curve with non-uniform cubic spline curves. Sulcal depth was similarly defined as the average length of 100 curves uniformly placed along the sulcal surface, perpendicular to the sulcal fundus and its top ridge. These curves were calculated by fitting the gradient of the isothermal lines, along the direction normal to fundus/

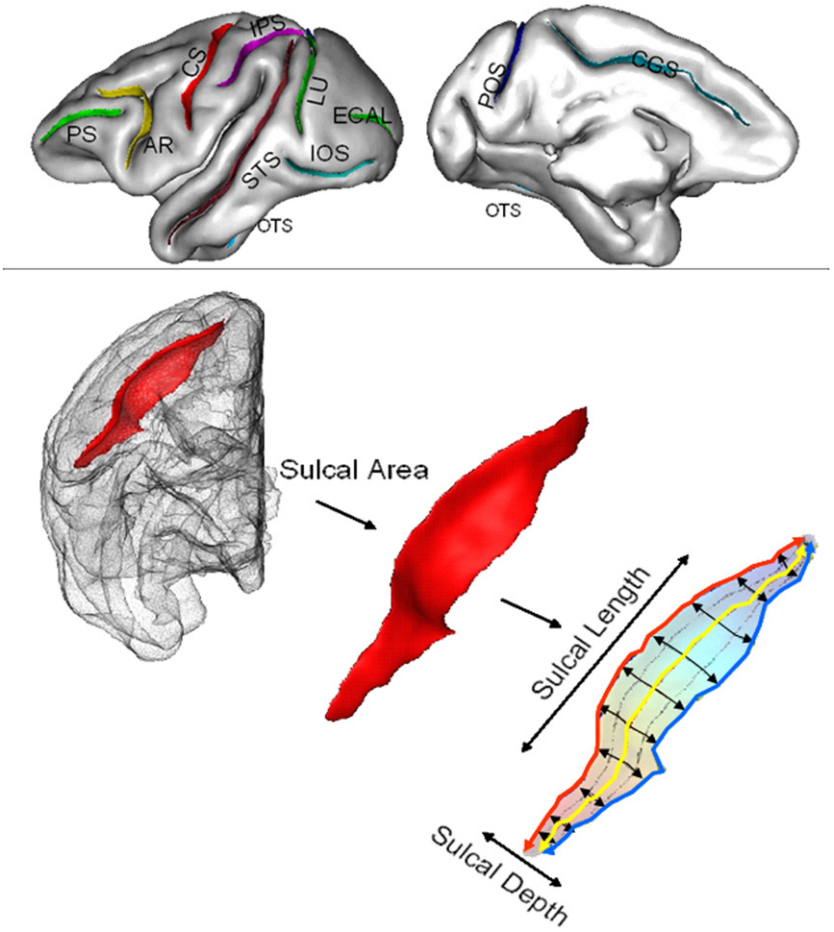


**Fig. 2.** Top panel: eleven cortical sulci were used in this analysis (Table 1). Bottom panel: A sulcal surface for the central sulcus is shown on a transparent cortical mesh (top). Three measurements were performed for each sulcal structure. The composite measurement sulcal area was measured as the surface area of the sulcal surface (middle). To compute two linear measurements, sulcal depth and length, sulcal surface was parameterized using a heat diffusion model. The length of the sulcus was measured as the average length of 100 isothermal lines fitted along the sulcal surface, continuously collinear with the fundus and the top ridge (three lines are shown in red, yellow and blue). Sulcal depth was calculated as the average length of 100 isothermal lines, along the sulcal surface, between the sulcal fundus and its top ridge (black lines).

top ridge, with non-uniform cubic spline curves throughout the sulcal surface (Fig. 2). Sulcal measurements were performed in both brain hemispheres and interhemispheric average values for sulcal area, length and depth were subjected to genetic analysis. The computational tools used for performing morphological sulcal measurements are available at http://ric.uthscsa.edu/personalpages/petr/.

*Selection and labeling of sulcal structures*

Eleven prominent primary sulcal structures were selected for this experiment. Cerebral sulci were named and labeled based on the schema from a combined histological/MRI rhesus brain atlas developed by Saleem and Logothetis (2007) (see Table 1 and Fig. 2, top). Cerebral sulci used in this study included all the primary sulci in a baboon brain, with the exclusion of the Sylvian fissure whose medial boundary extractions was unreliable. Sulcal phenotypes were averaged for both hemispheres to reduce the number of dependent measurements.

*Quantitative genetic analysis of sulcal phenotypes*

Variance components methods, as implemented in the Sequential Oligogenic Linkage Analysis Routines (SOLAR) software package (http://solar.sfbrgenetics.org) (Almasy and Blangero, 1998), were used to estimate the heritability of measured traits. The algorithms in SOLAR employ maximum likelihood variance decomposition methods and are an extension of the strategy developed by Amos (1994). Briefly, the covariance matrix $\Omega$ for a pedigree of individuals is given by Eq. (2).

$$\Omega = 2\Phi\sigma_g^2 + I\sigma_e^2 \quad (2)$$

where the $\sigma^2_g$ is the genetic variance due to the additive genetic factors, $\Phi$ is the kinship matrix representing the pair-wise kinship coefficients among all animals, $\sigma^2_e$ is the variance due to individual-specific environmental effects, and $I$ is an identity matrix. The kinship matrix ($\Phi$) is calculated based on the known breeding records and is confirmed with molecular genetic testing that identifies parent-offspring relationships among baboons. This produces a multigenerational pedigree that summarizes the genetic relationships among all individuals. For additional explanation of the variance components approach in this context, see Almasy and Blangero (1998) and Blangero et al. (2001).

Heritability ($h^2$), the portion of phenotypic variance ($\sigma^2_p$) that is accounted for by additive genetic variance (Eq. (1)), is assessed by contrasting the observed phenotypic covariance matrix with the covariance matrix predicted by kinship. Significance of heritability is tested by comparing the likelihood of the model in which $\sigma^2_g$ is constrained to zero with that of a model in which $\sigma^2_g$ is estimated. Twice the difference between the two $\log_e$ likelihoods of these models yields a test statistic, which is asymptotically distributed as a 1/2:1/2 mixture of a $\chi 1^2$ variable and a point mass at zero. Prior to testing for the significance of heritability, phenotype values for each individual are adjusted for a series of covariates. In our analysis we used a polygenic model that estimated the influence of specific variables (additive genetic variation, and covariates including sex, age, age$^2$, age × sex interaction, age$^2$ × sex interaction and random unidentified environmental effects) calculating heritability and its significance ($p$-value) for each trait's variance within this population. The level of significance for the heritability analysis for individual sulci was set at $p \leq .001$ to reduce the probability of type 1 errors associated with multiple (11) measurements.

## Results

*Cortical phenotypes*

The average sulcal length for eleven structures was 39.8 ± 13.5 mm, with the superior-temporal sulcus (STS) being the longest at 72.5 ± 3.6 mm and the principal sulcus being the shortest at 26.1 ± 3.5 mm (Table 1). The average depth of cortical sulci was calculated at 10.9 ± 4.0 mm, with STS being the deepest at 17.8 ± 1.0 mm and occipital-temporal sulcus being the shallowest at 6.2 ± 1.5 mm. The average sulcal area was 598.3 ± 535.5 mm$^2$, with STS showing the largest surface area at 1237.8 ± 102.1 mm$^2$ and external-calcarine (*ECAL*) sulcus showing the smallest area: 201.1 ± 64 mm$^2$. Sulcal area was highly correlated with both length and depth (Pearson's $r = \sim.8$; $p < .01$). This is expected, as the area depends on the length and depth. However, sulcal depth and length were not significantly correlated (Pearson's $r = .15$; $p = 0.7$).

*Genetic analysis of cortical phenotypes*

On average, ~40% of the morphological variability in sulcal area, depth and length was attributed to genetic variation (Table 2). All eleven sulci showed a significant heritability at the level of $p < .05$ for at least one of the measurements; however, only the central sulcus showed significant heritability at the level of $p < .001$ for all three measurements (Table 2). Gender, age and age$^2$ were among the significant covariates explaining on average about 6% of phenotypic variability. There were no significant age by sex and age$^2$ by sex interactions for any of the phenotypes. The heritability pattern for sulcal area was significantly correlated with the heritability patterns for sulcal depth (Pearson's $r = .71$; $p = .02$) and length (Pearson's $r = .61$; $p = .05$). Heritability patterns for the length and depth measurements were not significantly correlated with each other (Pearson's $r = .25$; $p = .5$).

Heritability of sulcal measurements varied by region and by phenotype. Sulcal area and depth measurements produced the largest

**Table 2**
Heritability ± standard error, the proportion of the total variance explained by covariates, and $p$-values are shown for sulcal area, depth, and length for 11 primary cortical sulci. The bolded heritability values were significant at the level of $p \leq .001$. Pattern of significant ($p \leq .001$) covariates was coded as [a](sex), [b](age), [c] (age$^2$).

| Sulcal name (Label) | Area | Depth | Length |
|---|---|---|---|
| Arcuate (ar) | .21 ± .11, .05 (.05) | .34 ± .14.06[a] (.01) | .11 ± .14, .03 (.20) |
| Cingulate (cgs) | .16 ± .15, .09[a,b] (.06) | .37 ± .24, .08[b] (.05) | .09 ± .12, .04 (.20) |
| Central (cs) | **.92 ± .15, .03 (1e−11)** | **.99 ± .11, .03 (1e−10)** | **.52 ± .19, .03 (1e−8)** |
| External-Calcarine calcarine (ecal) | **.59 ± .20, .06 (1e−3)** | .55 ± .21, .04 (.01) | **.50 ± .18, .06 (1e−3)** |
| Inferior occipital (ios) | **.49 ± .20, .14[a,c] (1e−3)** | .28 ± .19, .08[a,c] (.06) | **.67 ± .22, .16[a,c] (1e−3)** |
| Occipital-temporal (ots) | .30 ± .15, .08[c] (.05) | .17 ± .11,0.04 (.01) | **.59 ± .21, .05 (1e−3)** |
| Inferior parietal (ips) | .15 ± .22, .07[a] (.30) | .12 ± .19, .07[a] (.12) | .20 ± .14, .05 (.03) |
| Parietal-occipital (pos) | .32 ± .15, .01 (.01) | .23 ± .16, .01 (.05) | .01 ± .19, .02 (.50) |
| Lunate (lu) | .22 ± .25, .07[a] (.20) | **.66 ± .20, .08[a,c] (1e−5)** | .31 ± .39, .01 (.50) |
| Principal (ps) | **.41 ± .16, .17[a,c] (1e−4)** | .30 ± .17, .12[a,c] (.01) | .49 ± .21, .12[a,c] (.01) |
| Superior-temporal (sts) | **.44 ± .17, .08[c] (1e−4)** | **.55** ± .22, .05 (**1e−3**) | .46 ± .18, .10[a,c] (.01) |

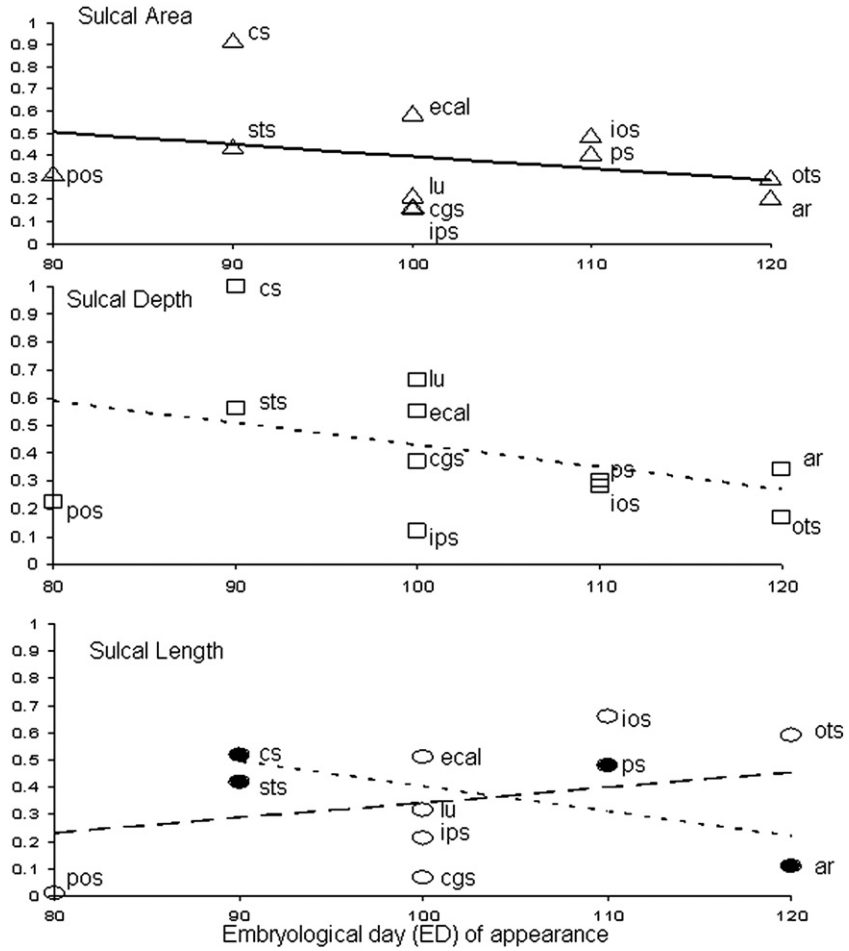


**Fig. 3.** Heritability for sulcal area (top, △, solid line), sulcal length (middle, ○, dashed line) and sulcal depth (bottom, □, dotted line) is plotted vs. embryological day of appearance. Heritability for sulcal length vs. ED plotted for 4 structures (filled markers, middle graph) used by Cheverud et al. shows a negative trend.

number of significantly heritable traits. For sulcal area, the highest heritability was observed for the central sulcus (*CS*) ($h^2 = .92$), which was followed by *ECAL* ($h^2 = .59$) and the lowest estimated heritability was seen for the *IPS* ($h^2 = .15$; $p = .3$). For sulcal depth, the highest heritability was also seen in the central sulcus where it approached 1.0 followed by the lunate (*LU*) and superior-temporal (*STS*) sulci ($h^2 = .66$ and .55; respectively, $p \leq .001$). The rest of the sulci did not show significant heritability at $p \leq .001$. The pattern of heritability for sulcal length was spatially diverse. Four sulci showed significant heritability values ($p \leq .001$) ranging from $h^2 = .67$ ($p < 1e{-}3$) for inferior occipital (*IOS*) to $h^2 = .50$ ($p = .03$) for external-calcarine sulcus (*ECAL*) (Table 2).

*Tests of a priori models*

Testing of two previously proposed models of regional differences in heritability in cortical morphology did not produce significant findings. To evaluate the first model, suggesting that heritability patterns are modulated by each structure's ontogenic age, the heritability values versus embryological day (ED) of appearance (Fukunishi et al., 2006; Kashima et al., 2008) were plotted (Fig. 3; Tables 1 and 2) No significant trend between heritability values and ED was detected for any of the sulcal phenotypes. The numerically highest correlation was seen for the sulcal length (Spearman's $\rho = .34$; $p = .3$). This trend was positive, indicating a higher genetic influence over developmentally later-appearing structures and therefore contrary to the original hypothesis. In our test of the second explanatory model, we observed no apparent relationship between heritability for sulcal phenotypes and the sulcal depth (Fig. 4; Table 3). Regional pattern of heritability for area and length was also independent of sulcal depth (Fig. 4). The numerically highest correlation (Pearson's $r = -.47$; $p = .2$) was observed between the heritability values for the sulcal length and the phenotypic sulcal depth. The sign of the correlation coefficient was opposite of what would be expected and its magnitude was not significant. We further investigated whether any of the sulcal phenotypic values, e.g., area, length and depth, were correlated with regional heritability values. The results, presented in Table 3, showed no apparent associations, indicating that average sulcal area, length and depth could not explain regional differences in heritability.

## Discussion

We measured the degree of genetic and environmental contributions to regional variability of sulcal area, length and depth and tested previously proposed theories of regional modulation of genetic influences by ontogenic and phenotypic factors. We found that the cortical phenotypes were moderately heritable with genetic factors explaining about 40% of intersubject differences and this was consistent with the typical heritability values reported for morphological traits (Mousseau and Roff, 1987). The regional pattern of heritability for cortical phenotypes was diverse and its variability results could not be explained by the two previously proposed models of genetic influences over gyrification.

We replicated some of the trends reported by the study by Cheverud and colleagues, even though their work examined rhesus macaques and we studied baboons. They calculated heritability of

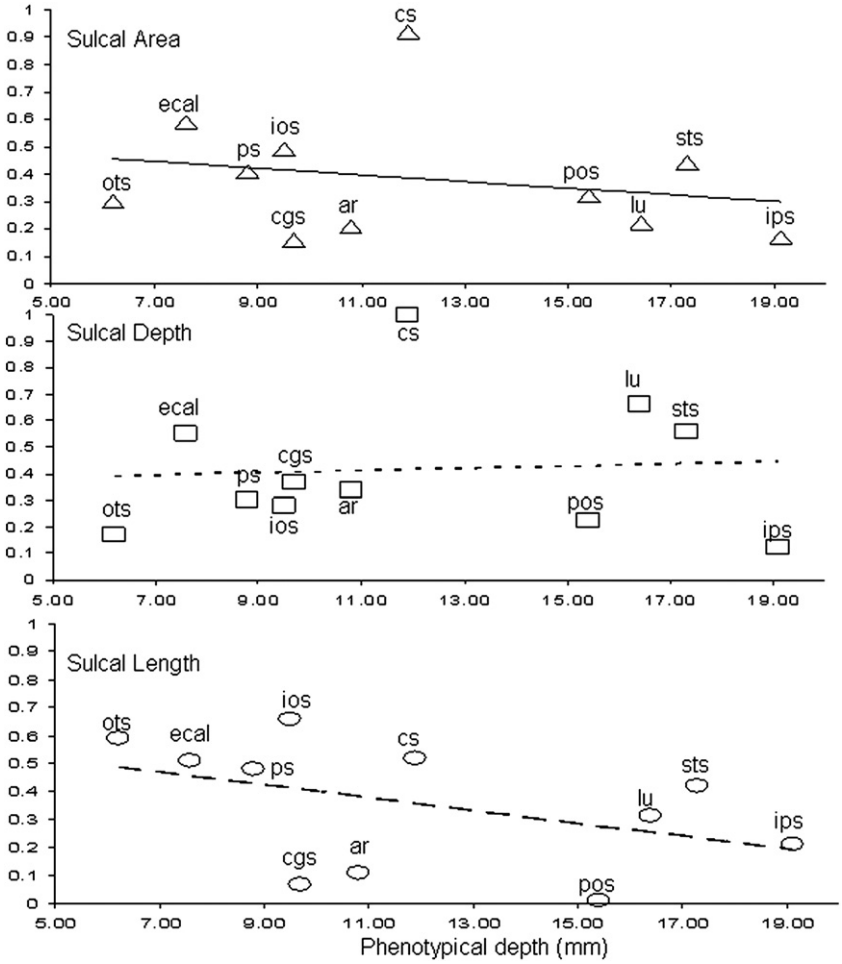


**Fig. 4.** Heritability for sulcal area (△, solid line), sulcal length (○, dashed line) and sulcal depth (□, dotted line) is plotted vs. sulcal depth for a given structure.

sulcal length for five cortical sulci, four of these sulci were included in our analysis (arcuate (*AR*), central (*CS*), principal (*PS*) and superior-temporal (*STS*)). The, fifth structure, Sylvian fissure, was excluded from our analysis for methodological reasons as its medial boundary could not be reliably extracted. Our findings for the average heritability of sulcal length ($h^2 = .34 \pm .21$) in baboons were similar to that reported for rhesus macaques by Cheverud and colleagues ($h^2 = .31$). In addition, the regional pattern of heritability values was also similar. Cheverud et al. provided heritability estimates for the length of *AR* ($h^2_L = .85$; $N_{pairs} = 65$), *CS* ($h^2 = .64$; $N_{pairs} = 76$), *PS* ($h^2 = .75$; $N_{pairs} = 66$), and *STS* ($h^2 = .46$; $N_{pairs} = 48$) (Cheverud et al., 1990).[1] We did not observe significant heritability for the length of *AR*. Nonetheless, heritability values for the remaining 3 sulci were highly similar. Cheverud et al. (1990) interpreted the regional differences in heritability as possibly being modulated by the ontogenic factors. Specifically they suggested that lower heritability values for cortical sulci appearing later during development could be due to increases in the variability of the prenatal hormone-mediated neurohumoral environment. Although we were able to replicate this trend in the subset of four sulci common to both analyses (*AR*, *CS*, *PS* and *STS*), where heritability estimates showed a trend toward a decline with advancing embryological day of appearance, this relationship was not statistically significant (Spearman's $\rho = -.63$, $p = 0.37$) (Fig. 3, middle). In addition, this trend was not present in the full set of sulci in our study where the correlations between ED and heritability of sulcal length were positive but non-significant ($r = \sim.4$; $p = .5$), therefore rejecting this model (Fig. 4, middle). This finding suggests that the genetic contribution to the variability of cortical phenotypes was not modulated by the ontogenic order of their appearance. Some developmental biologists have suggested that earlier appearing structures will be more tightly controlled by genetic factors during development, thus leading to higher heritabilities. However this assertion is not consistent with our results nor those of others who note that the earliest developing structures are clearly evolvable through the course of the evolutionary history (Raff, 1996), and may be susceptible to environmental perturbations.

We were also unable to replicate the findings of Lohmann and colleagues (1999, 2007) who suggested that deeper sulci have higher heritability values. The highest heritability in sulcal depth was observed for *CS* ($h^2 = .99$, $p = 10^{-10}$; average depth $= 11.9 \pm .7$ mm) and the heritability of the depth for the deepest sulcus, *IPS*, was not significant ($h^2 = .12$, $p = .12$; average depth $= 19.1 \pm 1.6$ mm). Our exploration showed that of the heritability values for none for

**Table 3**
Correlation between heritability ($h^2$), the proportion of total variance explained by genetic factors), and average values for area, depth and length for eleven primary sulci.

| Phenotype | $h^2$ Area | $h^2$ Length | $h^2$ Depth |
|---|---|---|---|
| Average area | −0.08 | −0.25 | 0.23 |
| Average depth | −0.23 | −0.47 | 0.08 |
| Average length | −0.03 | −0.07 | 0.08 |

[1] Heritability estimates for 5 sulci were calculated by averaging heritability values for each hemisphere. $N_{pair}$ refers to the reported number of mother–offspring pairs used in calculation of heritability values.

phenotypic measurements (e.g., area, length or depth) appeared to be significant modulated by sulcal depth (Fig. 4; Table 3). Our findings suggested that the regional pattern of genetic contribution to the variability of cortical landscape was more complex than previously suggested. Neither developmental nor phenotypic factors were able to explain the regional differences in heritability of sulcal phenotypes.

Estimated heritability for the central sulcus' (*CS*) depth and area approached 100%, yet the heritability of its length was only half of that figure. The central sulcus is a unique cortical structure, which consistently separates the frontal and parietal lobes in all gyrencephalic primates, including humans (Tamraz and Comair, 2006). The fundus (bottom ridge) of *CS* draws a distinct boundary between primary motor and primary sensory cortices separating functional areas BA4 and BA3-1-2. Another interesting morphological feature of *CS* is an intricate system of short white matter associative fibers, known as U-fibers, arching under the floor of the sulcus and connecting the opposing primary motor and sensory cortices (Boling et al., 2008; Cykowski et al., 2008a). Higher heritability values for depth versus length were observed in four other sulci (*CGS*, *IPS*, *LU*, *POS* and *STS*) that are known to separate distinct cyto- and myeloarchitectural areas and that have well developed U-fiber system. As a group these four sulci had heritability values for depth about twice as high as heritability values for length ($h^2_{\text{Depth}} = .38 \pm .22$ vs. $h^2_{\text{Lenght}} = .21 \pm .17$); however, this difference only approached significance (paired two-tailed *t*-test, $t = 2.2$, $p = .09$).

In contrast, sulci surrounded by cortex with similar myelo- and microarchitectonic areas showed higher heritability for length rather than depth. For sulci such as *ECAL*, *IOS*, *OTS* and *PS*, the average heritability for sulcal length was about twice as high as heritability for sulcal depth ($h^2_{\text{Lenght}} = .59 \pm .08$ vs. $h^2_{\text{Depth}} = .32 \pm .16$). Again, this difference was not significant (paired two-tailed *t*-test, $t = 2.1$, $p = .11$). Sulci that are enveloped by similar functional areas are characterized by the U-fiber white matter connection pattern that generally does not link opposing gyral banks, but rather extends to nearby gyri (Schmahmann and Pandya, 2006). It is tempting to suggest that the differences in the gyral white matter connection patterns may explain some portion of the regional differences in heritability. However, we are unable to directly test this hypothesis as cortical sulci, other than the central sulcus, are of a mixed type as they express both types of U-fibers along their course. For example, the superior branch of *AR* is enveloped by the area BA8 with U-fiber tracts extending in the superior and inferior directions (Schmahmann and Pandya, 2006). In contrast, its inferior branch, which separates BA45 on the anterior aspect from BA44 and 47 on the posterior aspect, has a well developed U-fiber system connecting the neighboring gyral banks (Schmahmann and Pandya, 2006). The direct test of this hypothesis would require a dataset describing regional variations in individual patterns of short and long distance white matter connection, such as high-resolution diffusion tensor imaging data. Further research that incorporates this data along with markers of cortical morphology is needed for a conclusive genetic study of cerebral gyrification.

### *Methods and limitations*

Our study was performed in baboons (*Papio hamadryas*). Our choice of experimental animals introduced two limitations. The first limitation is that the hypothesis regarding the modulation of the heritability of the sulcal length by developmental factors was tested using the ontogenic measurements from cynomolgus monkeys (*Macaca fascicularis*) (Fukunishi et al., 2006; Kashima et al., 2008). Despite the fact that the ontogenetic order of sulcal structures being preserved among Old World primates (Armstrong et al., 1995), this is a limitation as the null hypothesis is being accepted based on a small number of sulci that appear within days of each other during primary gyrification. However, our preliminary data on the ontogeny of cerebral gyrification in baboons based on longitudinal *in utero* imaging of fetal brain development in baboons (*study in progress*) show a good concordance with the ontogenetic pattern reported for macaques. A second limitation is that our sulcal classification and the pattern of associated functional areas (Table 1) were based on data from rhesus macaques (Saleem and Logothetis, 2007). However, primary sulcal and gyral patterns are similar between these two species, and we felt that this again was a minor limitation.

## Conclusion

This work is an expansion of our previous research on genetics of brain morphology in nonhuman primates (Rogers et al., 2007). Here, we studied genetic contributions to regional morphological variability of cerebral cortex and evaluated two previously proposed models of genetic contribution to variability in cerebral sulcation. The first model, proposed by Cheverud and colleagues, was based on a concept that the morphology of earlier developing brain structures is more genetically predetermined. This model suggested that the structure's ontogenic age is a modulating factor for the fraction of morphological variability explained by genetic factors (Cheverud et al., 1990). The second model proposed by Lohmann and colleagues suggested that the morphology of deeper sulci is more genetically predetermined, with sulcal depth acting as a modulating factor of genetic contribution. Neither of these models was fully tested by their original authors due to methodological limitations. However, our results did not support either of these models. Although we replicated the trend of negative correlation between heritability and embryological age reported by Cheverud et al. in a subset of structures common to both studies, this trend was not observed in the complete dataset, where the sign of the correlation was opposite to what's predicted by the model, hence rejecting it. We were unable to replicate the finding of a high positive correlation between heritability and sulcal depth reported by Lohmann et al. (1999), therefore rejecting the second model. In the post-hoc analysis we observed that heritability of sulcal depth was higher than heritability of sulcal length for the sulci that separate distinct cyto- and myeloarchitectural areas. Interestingly, a contrasting relationship was observed for sulci enveloped by cortex with similar myelo- and microarchitectonic areas. These sulci showed higher heritability for length rather than depth. We suggested this could be an indication that the differences in the gyral white matter connection patterns may explain some portion of the regional differences in heritability. Further research that incorporates individual differences in white matter connections is needed for a genetic study of cerebral gyrification that can address the causes of differences in heritability across sulcal phenotypes and regions.

## References

Almasy, L., Blangero, J., 1998. Multipoint quantitative-trait linkage analysis in general pedigrees. Am. J. Hum. Genet. 62, 1198–1211.
Amos, C.I., 1994. Robust variance-components approach for assessing genetic linkage in pedigrees. Am. J. Hum. Genet. 54, 535–543.
Armstrong, E., Curtis, M., Buxhoeveden, D.P., Fregoe, C., Zilles, K., Casanova, M.F., McCarthy, W.F., 1991. Cortical gyrification in the rhesus monkey: a test of the mechanical folding hypothesis. Cereb. Cortex 1, 426–432.
Armstrong, E., Schleicher, A., Omran, H., Curtis, M., Zilles, K., 1995. The ontogeny of human gyrification. Cereb. Cortex 5, 56–63.
Blangero, J., Williams, J.T., Almasy, L., 2001. Variance component methods for detecting complex trait loci. Adv. Genet. 42, 151–181.
Boling, W., Parsons, M., Kraszpulski, M., Cantrell, C., Puce, A., 2008. Whole-hand sensorimotor area: cortical stimulation localization and correlation with functional magnetic resonance imaging. J. Neurosurg. 108, 491–500.
Brodmann, K., G.J., 2005. Brodmann's: localisation in the cerebral cortex, 1st ed. Springer.
Brun, C., Lepore, N., Pennec, X., Chou, Y.Y., Lee, A.D., Barysheva, M., de Zubicaray, G., Meredith, M., McMahon, K., Wright, M.J., Toga, A.W., Thompson, P.M., 2008. A tensor-based morphometry study of genetic influences on brain structure using a new fluid registration method. Med. Image Comput. Comput. Assist. Interv. Int. Conf. Med. Image Comput. Comput. Assist. Interv. 11, 914–921.

Cheverud, J.M., Falk, D., Vannier, M., Konigsberg, L., Helmkamp, R.C., Hildebolt, C., 1990. Heritability of brain size and surface features in rhesus macaques (*Macaca mulatta*). J. Hered. 81, 51–57.

Chiang, M.C., Barysheva, M., Lee, A.D., Madsen, S., Klunder, A.D., Toga, A.W., McMahon, K.L., de Zubicaray, G.I., Meredith, M., Wright, M.J., Srivastava, A., Balov, N., Thompson, P.M., 2008. Brain fiber architecture, genetics, and intelligence: a high angular resolution diffusion imaging (HARDI) study. Med. Image Comput. Comput. Assist. Interv. Int. Conf. Med. Image Comput. Comput. Assist. Interv. 11, 1060–1067.

Coulon, O., Clouchoux, C., Operto, G., Dauchot, K., Sirigu, A., Anton, J.-L., 2006. Cortical localization via surface parameterization: a sulcus-based approach. NeuroImage 31 (Suppl. 1), S46.

Cykowski, M.D., Coulon, O., Kochunov, P.V., Amunts, K., Lancaster, J.L., Laird, A.R., Glahn, D.C., Fox, P.T., 2008a. The central sulcus: an observer-independent characterization of sulcal landmarks and depth asymmetry. Cereb. Cortex 18 (9), 1999–2009.

Cykowski, M.D., Kochunov, P.V., Ingham, R.J., Ingham, J.C., Mangin, J.F., Rivière, D., Lancaster, J.L., Fox, P.T., 2008b. Perisylvian sulcal morphology and cerebral asymmetry patterns in adults who stutter. Cereb. Cortex 18 (3), 571–583.

Deichmann, R., Good, C., Josephs, O., Ashburner, J., Turner, R., 2000. Optimization of 3-D MP-RAGE sequences for structural brain imaging. NeuroImage 12, 112–127.

Fischl, B., Rajendran, N., Busa, E., Augustinack, J., Hinds, O., Yeo, B.T., Mohlberg, H., Amunts, K., Zilles, K., 2007. Cortical folding patterns and predicting cytoarchitecture. Cereb. Cortex.

Fornito, A., Malhi, G.S., Lagopoulos, J., Ivanovski, B., Wood, S.J., Velakoulis, D., Saling, M.M., McGorry, P.D., Pantelis, C., Yucel, M., 2007. In vivo evidence for early neurodevelopmental anomaly of the anterior cingulate cortex in bipolar disorder. Acta Psychiatr. Scand. 116, 467–472.

Fukunishi, K., Sawada, K., Kashima, M., Sakata-Haga, H., Fukuzaki, K., Fukui, Y., 2006. Development of cerebral sulci and gyri in fetuses of cynomolgus monkeys (*Macaca fascicularis*). Anat. Embryol. (Berl.) 211, 757–764.

Galaburda, A.M., Pandya, D., 1982. Role of achitechtonics and connections. In: Armstrong, E., Falk, D. (Eds.), Primate Brain Evolution: Methods and Concepts. Plenum, New York, pp. 203–216.

Harris, J.M., Whalley, H., Yates, S., Miller, P., Johnstone, E.C., Lawrie, S.M., 2004. Abnormal cortical folding in high-risk individuals: a predictor of the development of schizophrenia? Biol. Psychiatry 56, 182–189.

Hulshoff Pol, H.E., Schnack, H.G., Posthuma, D., Mandl, R.C., Baare, W.F., van Oel, C., van Haren, N.E., Collins, D.L., Evans, A.C., Amunts, K., Burgel, U., Zilles, K., de Geus, E., Boomsma, D.I., Kahn, R.S., 2006. Genetic contributions to human brain morphology and intelligence. J. Neurosci. 26, 10235–10242.

Kashima, M., Sawada, K., Fukunishi, K., Sakata-Haga, H., Tokado, H., Fukui, Y., 2008. Development of cerebral sulci and gyri in fetuses of cynomolgus monkeys (*Macaca fascicularis*). II. Gross observation of the medial surface. Brain Struct. Funct. 212, 513–520.

Kochunov, P., Duff Davis, M., 2010. Development of structural MR brain imaging protocols to study genetics and maturation. Methods. 50 (3), 136–146.

Kochunov, P., Mangin, J.F., Coyle, T., Lancaster, J., Thompson, P., Rivière, D., Cointepas, Y., Régis, J., Schlosser, A., Royall, D.R., Zilles, K., Mazziotta, J., Toga, A., Fox, P.T., 2005 Nov. Age-related morphology trends of cortical sulci. Hum. Brain Mapp. 26 (3), 210–220.

Kochunov, P., Lancaster, J., Glahn, DC., Purdy, D., Laird, AR., Gao, F., Fox, P., 2006 Dec. Retrospective motion correction protocol for high-resolution anatomical MRI. Hum. Brain Mapp. 27 (12), 957–962.

Le Goualher, G., Argenti, A.M., Duyme, M., Baare, W.F., Hulshoff Pol, H.E., Boomsma, D.I., Zouaoui, A., Barillot, C., Evans, A.C., 2000. Statistical sulcal shape comparisons: application to the detection of genetic encoding of the central sulcus shape. NeuroImage 11, 564–574.

Leigh, S.R., 2004. Brain growth, life history, and cognition in primate and human evolution. Am. J. Primatol. 62, 139–164.

Leigh, S.R., Shah, N.F., Buchanan, L.S., 2003. Ontogeny and phylogeny in papionin primates. J. Hum. Evol. 45, 285–316.

Lohmann, G., von Cramon, D.Y., Steinmetz, H., 1999. Sulcal variability of twins. Cereb. Cortex 9, 754–763.

Lohmann, G., von Cramon, D.Y., Colchester, A.C., 2007. Deep sulcal landmarks provide an organizing framework for human cortical folding. Cereb. Cortex.

Lohmann, G., von Cramon, D.Y., Colchester, A.C., 2008 Jun. Deep sulcal landmarks provide an organizing framework for human cortical folding. Cereb. Cortex 18 (6), 1415–1420.

Mangin, J.F., Frouin, V., Bloch, I., Régis, J., López-Krahe, J., 1995. From 3D magnetic resonance images to structural representations of the cortex topography using topology preserving deformations. J. Math. Imaging Vis. 5, 297–318.

Mangin, J.F., Riviere, D., Cachia, A., Papadopoulos-Orfanos, D., Collins, D.L., Evans, A.C., Regis, J., 2003. Object-based strategy for morphometry of the cerebral cortex. Inf. Process. Med. Imaging 18, 160–171.

Mangin, J.F., Rivière, D., Coulon, O., Poupon, C., Cachia, A., Cointepas, Y., Poline, J.B., Le Bihan, D., Regis, J., Papadopoulos-Orfanos, D., 2004. Coordinate-based versus structural approaches to brain image analysis. Artif. Intell. Med. 30, 77–97.

Martin, R.D., 1990. Primate origins and evolution. Princeton University Press, Princeton, NJ.

Martin, R.D., Soligo, C., Tavare, S., 2007. Primate origins: implications of a cretaceous ancestry. Folia Primatol. (Basel) 78, 277–296.

Mousseau, T.A., Roff, D.A., 1987. Natural selection and the heritability of fitness components. Heredity 59 (Pt. 2), 181–197.

Narr, K.L., Bilder, R.M., Kim, S., Thompson, P.M., Szeszko, P., Robinson, D., Luders, E., Toga, A.W., 2004. Abnormal gyral complexity in first-episode schizophrenia. Biol. Psychiatry 55, 859–867.

Neal, J., Takahashi, M., Silva, M., Tiao, G., Walsh, C.A., Sheen, V.L., 2007. Insights into the gyrification of developing ferret brain by magnetic resonance imaging. J. Anat. 210, 66–77.

Pillay, P., Manger, P.R., 2007. Order-specific quantitative patterns of cortical gyrification. Eur. J. Neurosci. 25, 2705–2712.

Preuss, T.M., 2007. Primate brain evolution in phylogenetic context. In: Kaas , J.H.a.P.,T.M. (Ed.), Evolution of Nervous Systems: Volume 4 Primates. Elsevier Academic Press, Boston, pp. 1–34.

Rademacher, J., Caviness Jr., V.S., Steinmetz, H., Galaburda, A.M., 1993. Topographical variation of the human primary cortices: implications for neuroimaging, brain mapping, and neurobiology. Cereb. Cortex 3, 313–329.

Rademacher, J., Burgel, U., Geyer, S., Schormann, T., Schleicher, A., Freund, H.J., Zilles, K., 2001a. Variability and asymmetry in the human precentral motor system. A cytoarchitectonic and myeloarchitectonic brain mapping study. Brain 124, 2232–2258.

Rademacher, J., Morosan, P., Schormann, T., Schleicher, A., Werner, C., Freund, H.J., Zilles, K., 2001b. Probabilistic mapping and volume measurement of human primary auditory cortex. NeuroImage 13, 669–683.

Raff, M., 1996. Neural development: mysterious no more? Science 274, 1063.

Rogers, J., Kochunov, P., Lancaster, J., Shelledy, W., Glahn, D., Blangero, J., Fox, P., 2007. Heritability of brain volume, surface area and shape: an MRI study in an extended pedigree of baboons. Hum. Brain Mapp. 28, 576–583.

Saleem, K., Logothetis, N., 2007. A combined MRI and histology atlas of the rhesus monkey brain. Elsevier, London.

Schmahmann, J., Pandya, D., 2006. Fiber pathways of the brain. Oxford University Press, New York.

Stewart, C.B., Disotell, T.R., 1998. Primate evolution—in and out of Africa. Curr. Biol. 8, R582–588.

Tamraz, J., Comair, Y., 2006. Atlas of regional anatomy of the brain using MRI: with functional correlations. Springer, New York.

Thompson, P.M., Cannon, T.D., Narr, K.L., van Erp, T., Poutanen, V.P., Huttunen, M., Lonnqvist, J., Standertskjold-Nordenstam, C.G., Kaprio, J., Khaledy, M., Dail, R., Zoumalan, C.I., Toga, A.W., 2001. Genetic influences on brain structure. Nat. Neurosci. 4, 1253–1258.

Thompson, P., Cannon, T.D., Toga, A.W., 2002. Mapping genetic influences on human brain structure. Ann. Med. 34, 523–536.

Van Essen, D.C., 1997. A tension-based theory of morphogenesis and compact wiring in the central nervous system. Nature 385, 313–318.

Van Essen, D.C., 2004. Surface-based approaches to spatial localization and registration in primate cerebral cortex. NeuroImage 23 (Suppl. 1), S97–S107.

Welker, W., 1990. Why does cerebral cortex fissure and fold? A review of determinants of gyri and sulci. A review of determinants of gyri and sulci. In: Comparative structure and evolution of cerebral cortex, Part II, vol 8B, New York.

Zilles, K., Armstrong, E., Moser, K.H., Schleicher, A., Stephan, H., 1989. Gyrification in the cerebral cortex of primates. Brain Behav. Evol. 34, 143–150.